A new mode for heme–heme interactions in hemoglobin associated with distal perturbations

Abraham Levy, Vijay S. Sharma,* Lu Zhang, and Joseph M. Rifkind
Molecular Dynamics Section, Laboratory of Cellular and Molecular Biology, National Institute on Aging, National Institutes of Health, Baltimore, Maryland 21224; and *Department of Medicine, University of California at San Diego, La Jolla, California 92093

ABSTRACT The distal side of the heme pocket, known to regulate ligand affinity, is shown to be directly involved in subunit interactions. Valency hybrids with oxygen or carbon monoxide bound to the reduced chain are used to model R-state hemoglobin with different distal perturbations. Electron paramagnetic resonance of the oxidized chains shows that the carbon monoxide perturbation is transmitted between subunits to the distal histidine and the oxidized iron center. A comparison of hybrids with only one type of chain oxidized and hybrids with a single $\alpha\beta$ dimer oxidized is consistent with this perturbation being transmitted across the $\alpha_1\beta_1$ interface. This represents a new mode of subunit interactions in hemoglobin.

INTRODUCTION

An understanding of subunit interactions between the four hemoglobin chains, and how these explain cooperative oxygen binding, has been the primary focus of hemoglobin research. Most of the emphasis in this area is based on the distinct differences between three-dimensional structures of deoxyhemoglobin (1) and fully liganded hemoglobin (2) determined by x-ray diffraction. The major structural differences (3) observed in the region of the heme involve movement of the iron into the heme plane and a change in the orientation of the proximal histidine. At the subunit interfaces, the major changes involve the carboxy termini salt bridges and the contacts at the equivalent $\alpha_1\beta_2$ and $\alpha_2\beta_1$ interfaces.

These results have been the basis for defining (4) a low-affinity T-state with a structure similar to that of deoxyhemoglobin and an high-affinity R-state with a structure similar to that of oxyhemoglobin. Cooperative oxygenation can be explained by a concerted two-state $T \rightarrow R$ transformation (5, 6, 7). Despite recent evidence for more than two states (8, 9,10, 11, 12–14), the structural analysis usually still focuses on the changes at the proximal side of the heme and at the $\alpha_1\beta_2$ interface (15), where the major structural changes are detected.

The configuration of the residues lining the distal side of the heme pocket, where molecular oxygen binds, are also altered by oxygenation, and are thought to play a role in controlling access of the ligand to the heme pocket. Nevertheless, the possibility of subunit interactions originating from or being transmitted via distal effects has for the most part been neglected (16).

To investigate this possibility we have used valency hybrids where the Fe^{2+} hemes of some of the chains are oxidized to Fe^{3+} and no longer bind oxygen. A comparison was made between valency hybrids with oxygen or carbon monoxide bound to the reduced chains. Although methemoglobin at low pH has some tendency to be in a T-like state, both of these liganded valency hybrids are expected to be in the high affinity R-state (17). The preferred linear orientation of carbon monoxide (18, 19) enhances the perturbation of the distal side of the heme by the ligand (20, 21) and produces ruffling of the porphyrin ring (19). However, the proximal histidine orientation and the $\alpha_1\beta_2$ contact are expected to be very similar for the oxygen and carbon monoxide valency hybrids.

A dramatic effect on the Fe^{3+} chains which do not bind either ligand thus demonstrates the transmission of primarily distal interactions in the R-state between subunits. A comparison of different hybrids implies that these interactions are transmitted through the $\alpha_1\beta_1$ interface.

MATERIALS AND METHODS

Preparation of hybrids

Valency hybrids with both α-chains oxidized ($\alpha^+\alpha^+\beta\beta$) or both β-chains oxidized ($\alpha\alpha\beta^+\beta^+$) were prepared according to previously published methods (22). The hybrid with a single ($\alpha\beta$) dimer oxidized was prepared by mixing a ten-fold excess of fully liganded hemoglobin with methemoglobin.

Because of dimer dissociation

$$(\alpha^L\beta^L)(\alpha^L\beta^L) \leftrightarrow 2(\alpha^L\beta^L) \quad (1)$$

$$(\alpha^L\beta^L)(\alpha^L\beta^L) + (\alpha^+\beta^+)(\alpha^+\beta^+) \leftrightarrow (\alpha^L\beta^L)(\alpha^+\beta^+) + (\alpha^L\beta^L)(\alpha^L\beta^L) \quad (2)$$

0006-3495/92/03/750/06 $2.00

with a ten-fold excess of the reduced hemoglobin nearly all of the oxidized chains exist as $(\alpha^L\beta^L)(\alpha^+\beta^+)$.

Because we only observe the oxidized chains by EPR methods, the observed EPR spectra in this system measure exclusively the properties of the hybrid $(\alpha^L\beta^L)(\alpha^+\beta^+)$.

Electron paramagnetic resonance (EPR)

X-band EPR spectra were measured using an IBM ER—200D-SRC spectrometer with 100-KHz modulation. A liquid transfer HeliTran cryogenic unit (model LTD-3-110, Air Products and Chemicals, Inc., Allentown, PA) in conjunction with an APD-E temperature controller was used to regulate the temperature in the EPR cavity to 12 K. Diphenylpicryl-hydrazyl (DPPH) was implemented as a *g*-marker.

4-mm OD quartz tubes (Wilmad Glass Co., Buena, NJ) were utilized as EPR sample holders. The samples were frozen by submerging the EPR tubes into liquid nitrogen. A thin polyethylene tube sealed at the bottom was inserted into the sample to prevent breakage of the tube when the aqueous sample expands during freezing. The EPR samples were stored in liquid nitrogen. Incubation at 233 K was performed in an external bath. After specified incubation times the EPR sample tube was placed in the EPR cavity being maintained at 12 K.

RESULTS AND DISCUSSION

Electron paramagnetic resonance (EPR) of the Fe^{3+} chains turns out to be a particularly sensitive way to probe the heme environment. As seen from Fig. 1, five distinct states of the oxidized chains are observed (*T*, *R*, *A*, *B*, *C*). The dominant complex is the high-spin tetragonal water complex, $(T{:}T_1, T_2)$ with $g_\perp = 6.0$ and

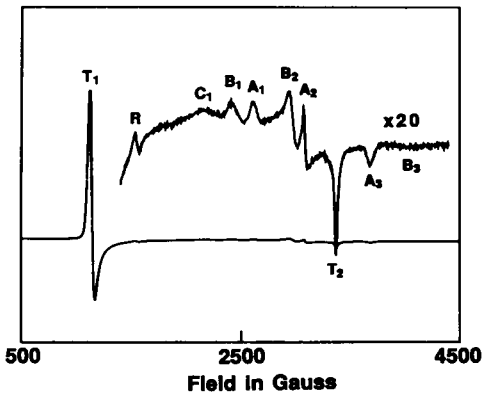

FIGURE 1 EPR spectrum of methemoglobin at pH 7.6. The samples were frozen by submerging the EPR tubes into liquid nitrogen. T_1, T_2 are $g_\perp$ and g_{11} components of the tetragonal high-spin complex, respectively. *R* represents signal of the rhombic high-spin complex; A_i, B_i, C_i are signals originating from the low-spin rhombic complexes *A*, *B*, and *C*. Each of these low-spin complexes have 3 *g*-values, g_1, g_2, and g_3, represented by the *i*'s.

$g_{11} = 2.0$. A minor high-spin rhombic complex is also detected with the only observed line at $g = 4.3$.

The low-spin hydroxide complex $(A{:}A_1, A_2, A_3)$ with $g_1 = 2.59, g_2 = 2.17$, and $g_3 = 1.83$ becomes the dominant species at higher pH's. Also detected are two low-spin complexes, *B* and *C*, which have been assigned (23) to low-spin bis-histidine complexes. Complex *B* $(B{:}B_1, B_2, B_3)$ with $g_1 = 2.83, g_2 = 2.26$, and $g_3 = 1.63$ is found even in methemoglobin frozen by freeze-quenching where the formation of new complexes during the freezing process is minimized. The $g_1 = 2.98$ has been attributed to a more stable bis-histidine complex (*C*) which is generally not detected when samples are frozen by freeze-quenching. For this complex, the EPR spectral line C_2 overlaps B_2 and C_3 is not detected. Complex *C* becomes a major component during incubation in the 210–250°K temperature range, during which time this complex grows at the expense of both high-spin and low-spin complexes (23).

The dependence of the transformation rate among the various species on the temperature of incubation is regulated exponentially by the energy barriers separating the different heme pocket configurations. Because of this functional dependence minor alterations in the heme pocket geometry, which can cause small changes in these energy barriers, are readily discernible by monitoring the transformation rate between the various subconformations at the proper temperatures, even when the immediately frozen samples have the same EPR spectra. For this reason the interconversion rate in the 210–250°K temperature range was measured to observe heme pocket alterations which might not be detected by other methods.

Transmission of distal interactions between hemoglobin chains

Although no perturbation was detected in the immediately frozen samples (Figs. 2 and 3), the technique of low temperature incubation (23) was able to characterize conformational changes transmitted from reduced chains to oxidized chains in the liganded valency hybrids. A series of EPR spectra of the oxidized chains for the hybrid with both α-chains oxidized $(\alpha^+\beta^L)(\alpha^+\beta^L)$, illustrating the changes after various incubation times, are shown in both the region of the high-spin $g = 6$ line from 1,000–1,300 gauss (Fig. 2) and in the low-spin g_1 region from 1,800–2,800 gauss (Fig. 3). Spectra are shown with oxygen bound to the reduced chains and with carbon monoxide bound to the reduced chains. With oxygen bound the changes are similar to those found for methemoglobin (23) where the high-spin tetragonal complex and low-spin complex *B* decrease in intensity during incubation and complex *C* increases in intensity.

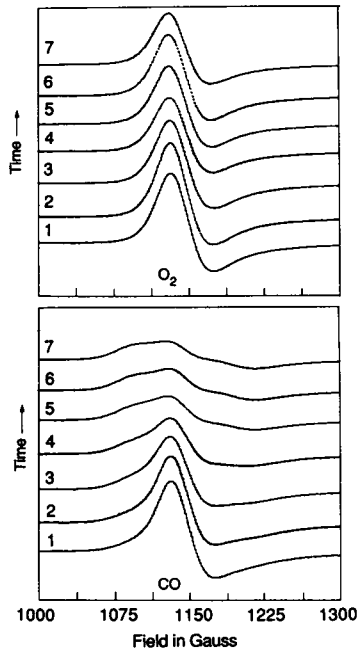

FIGURE 2 Effect of incubation at 233°K on the high-spin EPR spectrum (12°K, 0.01 M phosphate, pH 6.0) from 1,000 gauss to 1,300 gauss. (*Top*) The valency hybrid $(\alpha^{+}\beta^{02})$ $(\alpha^{+}\beta^{02})$ with both α-chains oxidized and oxygen bound to the reduced chains, and (*bottom*) the hybrid $(\alpha^{+}\beta^{\infty})$ $(\alpha^{+}\beta^{\infty})$ with both α-chains oxidized and carbon monoxide bound to the reduced chains. Before incubation, the EPR samples were stored in liquid nitrogen. Incubation at 233°K was performed in an external bath. After specified incubation times the EPR sample tube was placed in the EPR cavity. Incubation times: 1, 0 min; 2, 1 min; 3, 2 min; 4, 4 min; 5, 10 min; 6, 20 min; 7, 40 min.

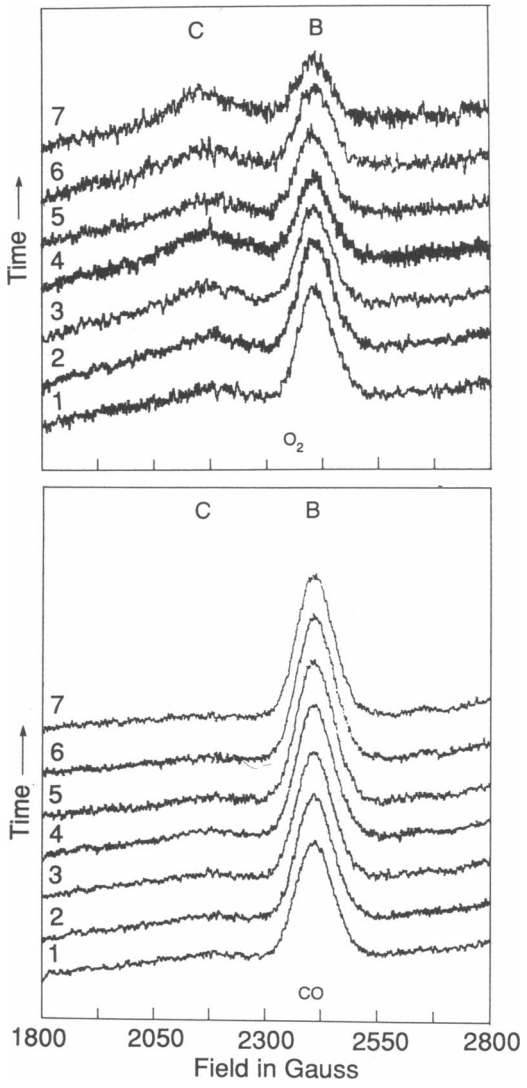

FIGURE 3 Effect of incubation at 233°K on the low-spin EPR spectrum (12°K, 0.01M phosphate, pH 6.0) from 1,800–2,800 gauss of the (*Top*) hybrid $(\alpha^{+}\beta^{02})(\alpha^{+}\beta^{02})$ with both α-chains oxidized and oxygen bound to the reduced chains, and (*Bottom*) the hybrid $(\alpha^{+}\beta^{\infty})(\alpha^{+}\beta^{\infty})$ with both α-chains oxidized and carbon monoxide bound to the reduced chains. Incubation times: 1, 0 min; 2, 1 min; 3, 2 min; 4, 4 min; 5, 10 min; 6, 20 min; 7, 40 min.

However, the replacement of oxygen by carbon monoxide produces a dramatic change in the spectra obtained after incubation. In the high-spin region (Fig. 2), the decreased intensity is more dramatic and the residual high-spin complex (*T*) shows a splitting of the $g = 6$ line indicative of a loss in tetragonal symmetry. In the low-spin region (Fig. 3) no complex *C* is formed and an increase in complex *B* is observed instead of the decrease found with oxygen. Similar effects are observed for the hybrid with both β-chains oxidized (Fig. 4).

The time-dependent changes observed when oxygen is replaced by carbon monoxide on valency hybrids are attributed to a change in the distribution of available substates for the distal histidine in the ligand pocket. This conformational perturbation, distinct from that observed for the changes in quaternary conformation, is not resolved in a static measure of conformation, but does, nevertheless, reflect significant differences in pocket dynamics.

From our studies on methemoglobin (23), complex *B* has been assigned to a configuration of the distal histidine which is compatible with the water molecule remaining in the ligand pocket, while complex *C* requires the removal of the water from the ligand pocket. At low temperature, the "driving force" for the redistribution of subconformations is the favorable energetics for interactions of the distal histidine with the iron and/or the H_2O bound to the Fe^{3+} chain.

With oxygen bound on the reduced chains the observed redistribution with a decrease of components *B* and *T* and formation of component *C* has been attrib-

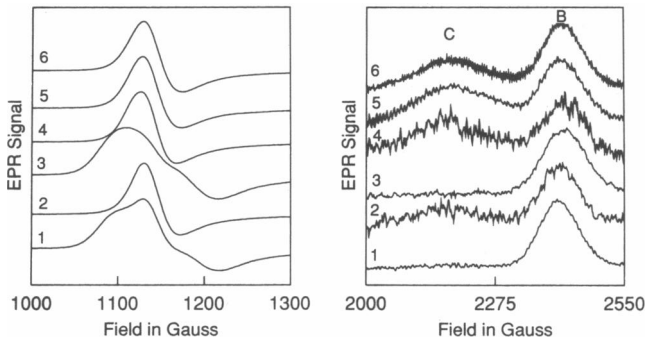

FIGURE 4 A comparison for different valency hybrids of the EPR spectra (12°K, 0.01 M phosphate, pH 6.0) obtained after incubation at 233°K. 1, $(\alpha^{+}\beta^{\infty})(\alpha^{+}\beta^{\infty})$; 2, $(\alpha^{+}\beta^{02})$ $(\alpha^{+}\beta^{02})$; 3, $(\alpha^{\infty}\beta^{+})(\alpha^{\infty}\beta^{+})$; 4, $(\alpha^{02}\beta^{+})(\alpha^{02}\beta^{+})$; 5, $(\alpha^{+}\beta^{+})(\alpha^{\infty}\beta^{\infty})$; 6, $(\alpha^{+}\beta^{+})(\alpha^{02}\beta^{02})$. (*Left*) The high-spin region of the EPR spectra from 1,000–1,300 gauss. (*Right*) The low-spin region of the EPR spectrum from 2,000–2,550 gauss.

uted to the H_2O leaving the pocket and the distal histidine binding to the iron (23). With carbon monoxide instead of oxygen, no complex *C* is observed, suggesting a more closed pocket on the oxidized chains with a higher energy barrier for the transformation from complex *B* to *C* which inhibits the escape of water from the pocket.

Even within the perturbed pocket found for the carbon monoxide hybrid, the distal histidine approaches the heme as a function of time at these low temperatures. This rearrangement of the ligand pocket causes two types of perturbations observed in the EPR spectrum. The orientation of the aqueous ligand is distorted, but remains bound, producing the high-spin complex with a loss of tetragonal symmetry (Figs. 2 and 4). Alternatively, the distal histidine displaces the aqueous ligand from the iron producing more of low-spin complex *B* (Figs. 3 and 4).

A perturbation of the oxidized chain in the deoxy valency hybrids which exist in the T-state has been reported for immediately frozen samples (17). However, for the valency hybrids with oxygen or carbon monoxide bound, no perturbation of the oxidized chain is observed in the immediately frozen samples. Both of these hybrids must therefore be in an R-like conformation analogous to those of oxyhemoglobin (2) and carbon monoxy hemoglobin (18, 19). The major differences in the x-ray structures of these two hemoglobins are increased heme ruffling (19) and perturbation on the distal side of the heme, both of which are associated with the preferred linear orientation of carbon monoxide. A comparison of the x-ray data with different distal ligands in the R-state indicates that these perturbations are transmitted to the *B*, *D*, *G*, and *H* helices (20).

In the valency hybrids $(\alpha^{+}\beta^{L})(\alpha^{+}\beta^{L})$ and $(\alpha^{L}\beta^{+})(\alpha^{L}\beta^{+})$ any perturbation of the oxidized chains associated with the replacement of oxygen by carbon monoxide must therefore be triggered by distal rearrangements and/or the ruffling of the porphyrin.

The role of distal interactions in regulating both the kinetics and thermodynamics for the binding of ligands has been extensively studied (24–28). However, the contribution of distal effects to subunit interactions in hemoglobin has been neglected (16). These valency hybrid studies provide the first indication that distal effects can be transmitted between hemes on different subunits which are separated by 25 Å across the $\alpha_1\beta_2$ interface and/or 40 Å across the $\alpha_1\beta_1$ interface.

Transmission of distal interactions across the $\alpha_1\beta_1$ interface

Evidence for the pathway for transmission of these distal perturbations was provided by comparing the hybrids where either both α-chains $(\alpha^{+}\beta^{L})(\alpha^{+}\beta^{L})$ or both β-chains $(\alpha^{L}\beta^{+})(\alpha^{L}\beta^{+})$ were oxidized with the hybrid where one of the αβ dimers were oxidized $(\alpha^{+}\beta^{+})(\alpha^{L}\beta^{L})$ (Fig. 4). No perturbation is found when oxygen is replaced by carbon monoxide in the hybrids with one αβ dimer oxidized (*Curves 5 and 6,* Fig. 4). For this hybrid, the results are very similar to that found for methemoglobin (23), i.e., the high-spin complex and low-spin *B* complex decrease in intensity during incubation with the formation of complex *C*.

In tetrameric hemoglobin the subunits are arranged in an irregular tetrahedron $\begin{matrix}\alpha_1\beta_2\\ \beta_1\alpha_2\end{matrix}$ with two distinct subunit contacts between α-chains and β-chains (3, 4). The $\alpha_1\beta_2$(or $\alpha_2\beta_1$) contact contains the region with major rearrangements when the x-ray structure of oxyhemoglobin is compared to that of deoxyhemoglobin (3). This interface contains both polar and nonpolar interactions involving the FG corner, the *C*-helix, and the carboxy terminal regions of both chains. The $\alpha_1\beta_1$(or $\alpha_2\beta_2$) interface contains extensive hydrophobic contacts involving parts of the *B*, *G*, and *H* helices as well as the GH corners of both chains. No changes in this interface are resolved by x-ray for ligand binding. However, it is important to note that the perturbations in the distal pocket have been shown to propagate as far as the *B*, *D*, *G*, and *H* helices (20), some of which are included in the $\alpha_1\beta_1$(or $\alpha_2\beta_2$) interface.

The comparison of both types of hybrids (Table 1) seems to require that the distal interactions are nevertheless transmitted across the $\alpha_1\beta_1$ (or $\alpha_2\beta_2$) interface. Thus, for $(\alpha^{+}\beta^{L})(\alpha^{+}\beta^{L})$ and $(\alpha^{L}\beta^{+})(\alpha^{L}\beta^{+})$ both types of interfaces are involved in contacts involving oxidized and reduced chains, and distortions are observed in the oxidized chains when oxygen is replaced by carbon

TABLE 1 **Contacts between oxidized and reduced chains for different valency hybrids**

Hybrid		Applicable interfaces	CO Perturbation
α-oxidized	$\alpha_1^+\beta_2$ $\beta_1\alpha_2^+$	$\alpha_1\beta_1$ and $\alpha_1\beta_2$	yes
β-oxidized	$\alpha_1\beta_2^+$ $\beta_1^+\alpha_2$	$\alpha_1\beta_1$ and $\alpha_1\beta_2$	yes
One (αβ) Dimer oxidized	$\alpha_1^+\beta_2$ $\beta_1^+\alpha_2$	only $\alpha_1\beta_2$	no

monoxide. However, for the hybrid $(\alpha^L\beta^L)(\alpha^+\beta^+)$, contact between oxidized and reduced chains involve only the $\alpha_1\beta_2$ interface, but not the $\alpha_1\beta_1$ interface, and no perturbation is observed when oxygen is replaced by carbon monoxide.

A possible role for the $\alpha_1\beta_1$ interface in ligand binding has been previously suggested (16). Ligand binding affects the SH vibration of the α-104 (G-11) cysteine residue in the $\alpha_1\beta_1$ interface (29) and the reaction of this cysteine residue with iodoacetamide (30) decreases the cooperativity for oxygen binding. Abnormal hemoglobins with modifications at the $\alpha_1\beta_1$ interface also alter oxygen affinity. Furthermore, cooperative binding of oxygen has been reported for the hybrid $(\alpha^{CN}\beta^{CN})(\alpha^{deoxy}\beta^{deoxy})$ where the two oxygens are binding to a single αβ dimer in tetrameric hemoglobin (31). However, these earlier studies do not provide the direct evidence for transmission made possible by the comparison of different valency hybrids. Furthermore, by comparing R-state hemoglobin with oxygen and carbon monoxide bound, it was possible to show that the $\alpha_1\beta_1$ transmissions are associated with distal perturbations and that the rearrangements of the $\alpha_1\beta_2$ interface associated with the T ↔ R transition are not required for transmission across the $\alpha_1\beta_1$ interface.

Relationship to ligand binding

A direct relationship between the subunit interactions altered by carbon monoxide in the EPR measurements and the ligand binding process has not been demonstrated. However, the demonstration of a distinct mode for subunit interactions being transmitted via the distal pocket across the $\alpha_1\beta_1$ interface may have relevance to the overall ligand binding properties of hemoglobin.

Although our results have focused on the R-state, within the T-state the ligand pocket is actually more constrained and distal perturbation associated with the binding of the first ligand to T-state hemoglobin may also be associated with subunit interactions transmitted across the $\alpha_1\beta_1$ interface. Clearly, further experimentation is required to demonstrate that such processes do occur within the T-state. Support for this hypothesis can however be provided by a number of published results. Thus, at least in the presence of inositol hexaphosphate at pH 6.94, the binding of carbon monoxide to HbA_0 is more cooperative than that of oxygen (32). Furthermore, using the method of modulated excitation to study the properties of triliganded hemoglobin (33) it has been shown that carbon monoxide alters the allosteric kinetics and equilibria.

A number of recent studies demonstrate that hemoglobin function can not be explained in terms of a ligand induced all or none quaternary transformation from T to R. Thus, many hemoglobin properties change after the first ligand is bound before the T to R quaternary transformation (8, 9, 34, 35). An altered T-state has actually been postulated to explain oxygen binding in the presence of organic phosphates (36).

The requirement for a thermodynamically relevant third structure in hemoglobin has been made on the basis of a detailed analysis of the energetics of subunit assembly (10, 14, 15). Consistent with a role for $\alpha_1\beta_1$ interactions, these investigators (14) have also found that the hybrid with both subunits of a single dimer liganded $(\alpha^L\beta^L)(\alpha\beta)$ is distinct from the hybrid where either both α-chains or both β-chains are liganded (see Table 1).

These observations seem to require a mode for heme–heme interaction to modulate hemoglobin function distinct from an all or none T ↔ R transformation. Distal effects which can be transmitted between subunits across the $\alpha_1\beta_1$ interface provide such a mode for heme–heme interaction. A mechanism for hemoglobin function is suggested, which combines modulation by distal interactions within αβ dimers and a rearrangement of the two dimers producing the changes in quaternary structure.

Received for publication 25 March 1991 and in final form 8 November 1991.

REFERENCES

1. Fermi, G., M. F. Perutz, B. Shaanan, and R. Fourme. 1984. The crystal structure of human deoxyhaemoglobin at 1.74 Å resolution. *J. Mol. Biol.* 175:159–174.
2. B. Shaanan. 1983. Structure of human oxyhaemoglobin at 2.1 Å resolution. *J. Mol. Biol.* 171:31–59.
3. Baldwin, J. and C. Chothia. 1979. Haemoglobin: the structural changes related to ligand binding and its allosteric mechanism. *J. Mol. Biol.* 129:175–220.
4. M. F. Perutz. 1970. Stereochemistry of cooperative effects of haemoglobin. *Nature (Lond.)*. 228:726–739.

5. Monod, J., J. Wyman, J. P. Changeux. 1965. On the nature of allosteric transitions: a plausible model. *J. Mol. Biol.* 12:88–118.
6. Gelin, B. R., and M. Karplus. 1977. Mechanism of tertiary structural change in hemoglobin. *Proc. Natl. Acad. Sci. USA* 74:801–805.
7. Gelin, B. R., A. W.-M. Lee, M. Karplus. 1983. Hemoglobin tertiary structural change on ligand binding. Its role in the cooperative mechanism. *J. Mol. Biol.* 171:489–559.
8. Hallaway, P. E., B. E. Hallaway, and A. Rosenberg. 1984. Study of hydrogen exchange in hemoglobin as a function of fractional ligand saturation. *Biochemistry.* 23:266–273.
9. Makino, N., and Y. Sugita. 1982. The structure of partially oxygenated hemoglobin. *J. Biol. Chem.* 257:163–168.
10. Smith, F. R., D. Gingrich, B. M. Hoffman, and G. K. Ackers. 1987. Three-state combinatorial switching in hemoglobin tetramers: comparison between functional energetics and molecular structure. *Proc. Natl. Acad. Sci. USA.* 20:7089–7093.
11. Fung, L. W.-M., A. P. Minton, and C. Ho. 1976. Nuclear magnetic resonance study of heme–heme interaction in hemoglobin Milwaukee: implications concerning the mechanism of cooperative ligand binding in normal hemoglobin. *Proc. Natl. Acad. Sci. USA.* 73:1581–1585.
12. Morris, R. J., Q. H. Gibson, M. Ikeda-Saito, and T. Yonetani. 1984. Geminate combination of oxygen with iron-cobalt hybrid hemoglobins. *J. Biol. Chem.* 259:6701–6703.
13. Hori, H., and T. Yonetani. 1986. Nonequivalence in the electronic structure of the prosthetic groups between two α-subunits within deoxycobalthemoglobin as determined by single-crystal EPR spectroscopy. *J. Biol. Chem.* 261:13693–13697.
14. Perella, M., L. Benazzi, M. A. Shea, and G. K. Ackers. 1990. Subunit hybridization studies of partially ligated cyanomethemoglobin using a cryogenic method. Evidence for three allosteric states. *Biophys. Chem.* 35:97–103.
15. Johnson, M. L., B. W. Turner, and G. K. Ackers. 1984. A quantitative model for the cooperative mechanism of human hemoglobin. *Proc Natl. Acad. Sci. USA* 81:1093–1097.
16. J. M. Rifkind. 1987. Hemoglobin. *In* Advances in Inorganic Biochemistry, Vol. 7. G. L. Eichhorn and L. G. Marzilli, editors. Elsevier/North Holland, New York. 155–244.
17. Nagai, K., and H. Hori. 1978. The influence of quaternary structure on the EPR spectra of ferric haemoglobin. *FEBS (Fed. Eur. Biochem. Soc.) Lett.* 93:275–277.
18. Baldwin, J. M. 1980. The structure of human carbonmonoxy haemoglobin. *J. Mol. Biol.* 136:103–128.
19. Derewenda, Z., G. Dodson, P. Emsley, D. Harris, K. Nagai, M. Perutz, and J. P. Reynaud. 1990. Stereochemistry of carbon monoxide binding to normal adult and Cowtown haemoglobins. *J. Mol. Biol.* 211:515–519.
20. Moffat, K., J. D. Deatherage, and D. W. Seybert. 1979. A structural model for the kinetic behavior of hemoglobin. *Science (Wash. DC).* 206:1035–1042.
21. Levy, A. 1989. Collective motion of iron and exogenous ligands in hemoglobin. *Biochemistry.* 28:7144–7147.
22. Sharma, V. S. 1988. Kinetic studies on partially liganded species of carboxyhemoglobin: $\alpha_2^{CO}\beta_2$ and $\alpha_2\beta_2^{CO}$. *J. Biol. Chem.* 263:2292–2298.
23. Levy, A., P. Kuppusamy, and J. M. Rifkind. 1990. Multiple heme pocket subconformations of methemoglobin associated with distal histidine interactions. *Biochemistry.* 29:9311–9316.
24. Olson, J. S., and Q. H. Gibson. 1972. The reaction of *n*-butyl isocyanide with human hemoglobin. II. The ligand binding properties of the α and β chains within deoxyhemoglobin. *J. Biol. Chem.* 247:1713–1726.
25. MacQuarrie, R., and Q. H. Gibson. 1972. Ligand binding and release of an analogue of 2,3-diphosphoglycerate from human hemoglobin. *J. Biol. Chem.* 247:5686–5694.
26. Ilgenfritz, G., and T. M. Schuster. 1974. Kinetics of oxygen binding to human hemoglobin. Temperature jump relaxation studies. *J. Biol. Chem.* 249:2959–2973.
27. Cassoly, R., and Q. H. Gibson. 1975. Conformation, cooperativity and ligand binding in human hemoglobin. *J. Mol. Biol.* 91:301–313.
28. Sharma, V. S., M. E. John, and M. R. Waterman. Functional studies on hemoglobin opossum. Conclusions drawn regarding the role of the distal histidine. *J. Biol. Chem.* 257:11887–11892.
29. Alben, J. O., and G. H. Bare. 1980. Ligand-dependent heme-protein interactions in human hemoglobin studied by Fourier transform infrared spectroscopy. Effects of quaternary structure on α-chain tertiary structure measured at the α-104 (G11) cysteine-SH. *J. Biol. Chem.* 255:3892–3897.
30. Waterman, M. R. 1976. Effect of carbamidomethylation of cysteine residues G11 (104)α on the properties of hemoglobin A. *Biochim. Biophys. Acta.* 439:167–174.
31. Imai, K. 1982. *Allosteric Effects in Hemoglobin.* Cambridge University Press.
32. DiCera, E., M. L. Doyle, P. R. Connelly, and S. J. Gill. 1987. Carbon monoxide binding to human hemoglobin A_0. *Biochemistry* 26:6494–6502.
33. Zhang, N., F. A. Ferrone, and A. J. Martino. 1990. Allosteric kinetics and equilibria differ for carbon monoxide and oxygen binding to hemoglobin. *Biophys. J.* 58:333–340.
34. Levy, A. and J. M. Rifkind. 1985. Low-temperature formation of a distal histidine complex in hemoglobin: a probe for heme pocket flexibility. *Biochemistry.* 24:6050–6054.
35. Sharma, V. S. 1983. Studies of human hemoglobin intermediates. The double mixing method for studying the reactions of the species $Hb_4(CO)$ and $Hb_4(CO)_2$. *J. Mol. Biol.* 166:677–684.
36. Goodford, P. J., J. St.-Louis, and R. Wootton. 1978. A quantitative analysis of the effects of 2,3-diphosphoglycerate, adenosine triphosphate and inositol hexaphosphate on the oxygen dissociative curve of human haemoglobin. *J. Physiol.* 283:397–407.